Relations between v_z and B_x components in solar wind and their effect on substorm onset

Marina Kubyshkina[1], **Vladimir Semenov**[1], **Nikolai Erkaev**[2,5], **Evgeny Gordeev**[1], **Stepan Dubyagin**[3], **Natalia Ganushkina**[3,4], **and Maria Shukhtina** [1]

[1]Saint Petersburg State University, Saint Petersburg, Russia.

[2]Institute of Computational Modelling, Federal Research Center 'Krasnoyarsk Science Center SB RAS', Russia

[3]Finnish Meteorological Institute, Helsinki, Finland.

[4]University of Michigan, Ann Arbor, MI, USA.

[5]Siberian Federal University, 660041 Krasnoyarsk, Russia.

Key Points:

- Using two substorm onset lists, we show that for 2/3 of all substorm onsets, the $(B_x \cdot v_z)$ product in the solar wind has the same sign as the IMF B_z-component.
- When the signs of the product $(B_x \cdot v_z)$ and the IMF B_z coincide, the asymmetry (bending) of the magnetotail current sheet increases.
- The $(B_x \cdot v_z)$ product in the solar wind during 2/3 of all the time has the sign of IMF B_z, which is a feature of Alfvénic waves propagating from the Sun.

Corresponding author: Marina Kubyshkina, m.kubyshkina@spbu.ru

Author Manuscript

Abstract

We analyze two substorm onset lists, produced by different methods, and show that the $(B_x \cdot v_z)$ product of the solar wind (SW) velocity and interplanetary magnetic field (IMF) components for 2/3 of all substorm onsets has the same sign as IMF B_z. The explanation we suggest is the efficient displacement of the magnetospheric plasma sheet due to IMF B_x and SW flow v_z, which both force the plasma sheet moving in one direction if the sign of $(B_x \cdot v_z)$ correlates with the sign B_z. The displacement of the current sheet, in its turn, increases the asymmetry of the magnetotail, and can alter the threshold of substorm instabilities.

We study the SW and IMF data for the 15-year period (which comprises two substorm lists periods and the whole solar cycle), and reveal the similar asymmetry in the SW, so that the sign of $(B_x \cdot v_z)$ coincides with the sign of IMF B_z during about 2/3 of all the time. This disproportion can be explained if we admit that about 66% of IMF B_z-component are transported to the Earth's orbit by the Alfvén waves with anti-sunward velocities.

1 Introduction

It is commonly accepted now that the existence of a southward component of Interplanetary Magnetic Field (IMF) is the main driver of magnetospheric activity [*Fairfield and Cahill*, 1966; *Rostoker and Falthammar*, 1967; *Akasofu*, 1975], since the southward direction of IMF is favorable for the magnetic reconnection at the magnetopause [*Dungey*, 1961]. Yet, the questions on when, why and how does the substorm expansion develop are still under discussion. One of the possible reasons for this long-lasting discussion is the great variability of substorms behavior and substorm onset configurations (see, for example, recent paper by *Borovsky and Yakimenko* [2017] and references therein.)

One of the important problems in this context is the existence of an external driver for substorm triggering. Recent study by *Newell et al.* [2016] demonstrated a clear dependence of substorm probability on the solar wind speed and claimed that the SW speed is the main predictor for substorm occurrence. That study also showed that any change in IMF B_z or SW speed increases the odds of a substorm if compared to no change, and, especially, if it is a drop in SW speed or a northward turn in IMF B_z. Both of these factors

slow down the rate of the magnetic field merging on the dayside magnetopause, but they do not significantly change the geometry of the magnetospheric configuration.

Our study stays somewhat aside from the mainstream of substorm research, we explore the solar wind flow v_z-component and the IMF B_x-component as the factors which change the rate of the asymmetry of magnetospheric configuration (see, for exapmle, [*Sergeev et al.*, 2008; *Hoilijoki et al.*, 2014; *Tsyganenko and Fairfield*, 2004]) and analyze how do they vary when approaching a substorm onset.

At present, there exist a few studies [*Panov et al.*, 2012; *Vörös et al.*, 2014; *Kubyshkina et al.*, 2015; *Semenov et al.*, 2015] which explore the substorm behavior in a situation with changing solar wind flow velocity. They show that fast changes in the solar wind flow v_z-component, especially in a situation with nonzero dipole tilt, may facilitate a substorm onset. A reason for that may be an additional curving and displacement of magnetospheric plasma sheet which lowers the substorm instability threshold in an asymmetric bent current sheet [e.g., *Kivelson and Hughes*, 1990].

However, the v_z-component of the flow velocity is not the only solar wind parameter which causes plasma sheet motion in the vertical (normal to ecliptic plane) direction. The existence of a nonzero B_x-component of IMF results in a displacement of an X-line for the dayside magnetopause reconnection and in the asymmetric magnetic flux circulation in magnetospheric lobes [*Cowley*, 1981; *Reistad et al.*, 2014; *Gordeev et al.*, 2016]. Magnetic flux imbalance in the northern and southern lobes leads, in turn, to the plasma sheet displacement from its equilibrium position. Depending on the sign of the B_x, the plasma sheet will move up or down in a similar way as it does due to a nonzero v_z-component of the SW flow.

Therefore, in the present paper, we investigate the mutual effect of both the SW flow v_z-component and the IMF B_x-component on substorm probability. Section 2 describes the details of motivation of this study, in Section 3 we study the pre-substorm statistics, in Section 4 we examine the solar wind and IMF data, and, finally, in section 5 we put together the results and discuss them.

2 Motivation details and background

The existence of the negative IMF B_z (here and below in this section we use Geocentric Solar Magnetic (GSM) coordinates) is one of the key requirements for a magneto-

78 spheric substorm initiation. Yet, it is also clear that there exist other factors which force

79 or slow down the substorm onset and vary the amount of energy stored during the growth

80 phase and released during the expansion phase.

81 If, based on previous works [*Kivelson and Hughes*, 1990; *Panov et al.*, 2012; *Kubyshk-*

82 *ina et al.*, 2015; *Semenov et al.*, 2015], we admit that the increased asymmetry of the mag-

83 netotail configuration lowers the threshold for substorm triggering instability, we need to

84 check how do the SW v_z-component and the IMF B_x-component change the position of

85 the magnetospheric plasma sheet.

86 Following the direction of the solar wind plasma flow, the magnetospheric plasma

87 sheet will move up from the ecliptic plane under positive solar wind flow velocity compo-

88 nent v_z and down under negative v_z, irrespective of the sign of the IMF B_z.
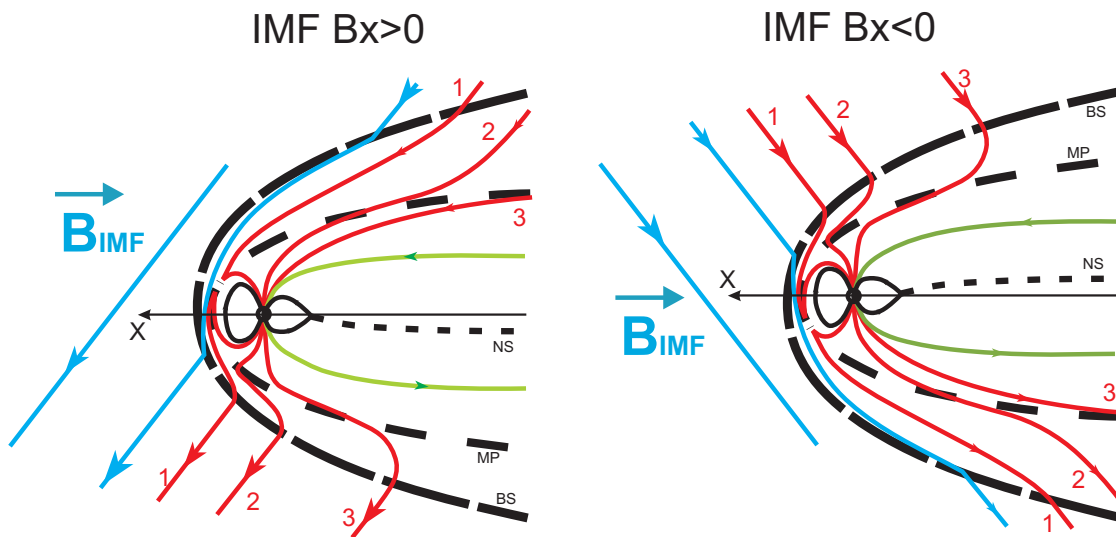

Figure 1. The directions of plasma sheet motion in the presence of positive (left) and negative (right) IMF

Bx component for southward IMF B_z. The blue lines correspond to IMF lines, the red lines are the recon-

nected magnetospheric-IMF lines, the green lines are Earth's magnetotail field lines. The thick black dashed

lines mark the position of Bow Shock (BS), Magnetopause (MP), and Neutral Sheet (NS)

93 The displacement of the plasma sheet under the nonzero IMF B_x is caused by the

94 non-symmetric dayside reconnection, when the X-line is shifted from the subsolar point.

95 As a result, the unbalanced reconnected magnetic fluxes in the southern and northern

96 magnetotail lobes force the plasma sheet moving up or down from the ecliptic plane (see

97 [*Cowley*, 1981; *Reistad et al.*, 2014; *Gordeev et al.*, 2016]). The rate of this displacement

will be large only under negative IMF B_z, when the dayside reconnection is active. This phenomenon is illustrated in Figure 1, adopted from *Cowley* [1981]. Under negative IMF B_z, the plasma sheet will move down with positive B_x-component, and plasma sheet will move up the equatorial plane with the negative B_x-component.

After we compare the plasma sheet reaction to the non-radial SW plasma flow and non-zero IMF B_x, we see that when IMF B_z is negative, the plasma sheet moves up with $B_x < 0$ and with $v_z > 0$, and the plasma sheet goes down with $B_x > 0$ and with $v_z < 0$. Thus, the rate and velocity of plasma sheet displacement will be maximal if the sign of a product $(v_z \cdot B_x)$ is the same as the sign of the B_z.

If the substorm onset happens under positive IMF B_z, usually it means that the IMF B_z changes its sign from negative to positive in a late growth phase. In this case, when the IMF B_z turns northward, the dayside reconnection stops and the previously (during the period with negative B_z) shifted plasma sheet starts to move in the opposite direction (up for B_x positive and down for B_x negative). Thus, the current sheet displacement due to the existence of the nonzero B_x and v_z will maximize if $(v_z \cdot B_x) > 0$, i.e., again , has the same sign as IMF B_z.

If we assume that the displacement of the plasma sheet is a favorable factor for a substorm onset, we would expect that a number of substorms, which start under the IMF B_z and $(v_z \cdot B_x)$ with the same signs should be larger than the number of substorms which start when the signs of the B_z and $(v_z \cdot B_x)$ are opposite.

3 Data analysis: Substorm Activity

To verify the above suggestion, we used the two principally different substorm databases:

1) the list of substorms from *Frey et al.* [2004], which is based on FUV data from IMAGE satellite and contains 4193 substorm onsets during 2000 to 2005;

2) the list of substorms from SUPERMAG ground-based magnetic observations (http: //supermag.jhuapl.edu/substorms/) based on automatic analysis of AL index behavior which contains 18807 substorm onsets during 2000-2010, the period which comprises the period of the *Frey et al.* [2004] data list and also includes both minimum and maximum of the solar cycle activity.

127 Each database was complemented with OMNI data, containing 5-minute values of

128 IMF and solar wind flow velocity for one hour preceding the substorm onsets. After that,

129 all the substorms were divided into two groups: those which started during southward B_z

130 ($B_z < -1$ nT) and those which began under northward B_z ($B_z > 1$ nT). We used only those

131 onsets, where OMNI data (for both magnetic field and solar flow) was available at the on-

132 set time. We excluded the near-zero values of B_z to avoid possible uncertainties, since the

133 sign of B_z is crucial for our analysis. For *Frey et al.* [2004] data the number of exclusions

134 with $-1 < B_z < 1$ was equal to 880 onsets (out of 3989 which had the OMNI data), and

135 for SUPERMAG data set we had 2966 exclusions (out of 18114 onsets with the OMNI

136 data).

137 The resulting distributions of a number of substorms with different $(v_z \cdot B_x)$ values

138 at the time of a substorm onset (5-min averaged values which precede 5-minutes period,

139 containing a substorm onset) are given in Figure 2 for both lists of substorms and in two

140 types of histograms: the two-column histogram gives the numbers of substorms with all

141 positive and all negative occurrences of $(v_z \cdot B_x)$, and the 20-column histogram shows a

142 more detailed distribution.

146 The top row of Figure 2 shows the discussed distributions only for the substorms,

147 which started under negative IMF B_z, with two histograms on the left for *Frey et al.* [2004]

148 substorm list and two histograms on the right for SUPERMAG substorm list. Both sub-

149 storm lists give the same imbalance in the number of substorms with different signs of

150 $(v_z \cdot B_x)$, the number of substorms which started under negative $(v_z \cdot B_x)$ is almost twice

151 (1.75 times) larger than the number of substorms which started under positive $(v_z \cdot B_x)$ (see

152 two-columns histograms in Figure 2a). Also, it is important to note, that this difference is

153 well reproduced in each pair of bins (positive and negative) of 20-columns histograms,

154 and becomes even larger for the larger values of $(v_z \cdot B_x)$ (see Figure 2a).

155 The bottom row of Figure 2 gives the same histograms for the substorms with the

156 onsets under positive IMF B_z ($B_z > 1$ nT). The total number of these substorms is much

157 smaller, their intensity is small on average, but the distributions are very similar, with al-

158 most twice overage of substorms which started under positive values of $(v_z \cdot B_x)$ (see two-

159 columns histograms in Figure 2b), and with more notable differences in substorm numbers

160 for larger values of $(v_z \cdot B_x)$ (see 20-columns histograms in Figure 2b).
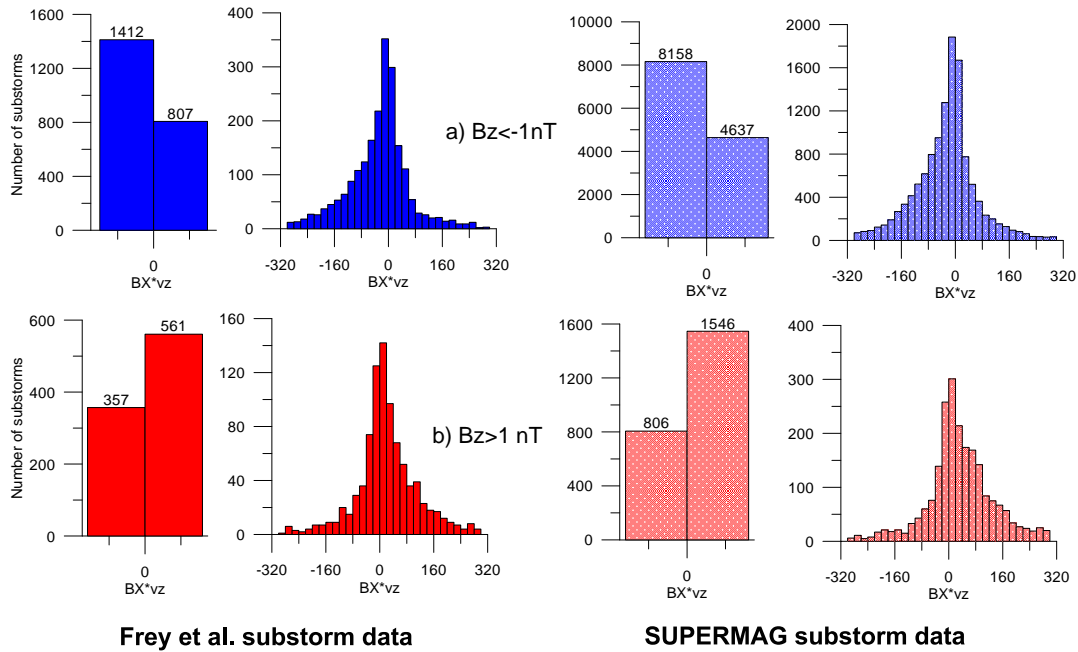
Figure 2. Histograms for the number of substorms with different values of $(v_z \cdot B_x)$, measured near the time of a substorm onset, for two substorm lists (on the right and on the left) and for both signs of IMF B_z (a and b - top and bottom).

The next important question is if the distribution which we observe near a moment of a substorm onset remains unchanged throughout the growth phase? To check it, we made the time series of 12 two-column histograms for both lists of substorms (the same as those in Figure 2) for twelve 5-min averaged points before the onset (for simplicity we used the same one-hour period as a growth phase for all the substorms). Using those histograms, we tracked how the relative number of the events for which $(v_z \cdot B_x)$ is positive/negative changes during the growth phase (or more precisely, during one hour before the substorm onset). The results are given in Figure 3. Each point on this plot is obtained as a relative difference (in percent) between the number of the events when $(v_z \cdot B_x)$ was negative at a given time before onset, and the number of the events when $(v_z \cdot B_x)$ was positive at the same time (i.e. the difference between 2 bins in the 2-columns histograms), normalized by the total number of substorms under the given sign of IMF B_z. Blue lines are used for the substorms which start under (B_z <-1 nT), and red lines - for

174   the substorms with the onsets under ($B_z > 1$ nT), the points from SUPERMAG database

175   are marked by crosses and the points for *Frey et al.* [2004] substorm database are marked

176   by triangles. Substorm onset is marked by zero on the horizontal axis. We see that the

177   difference between the number of events where the sign of ($v_z \cdot B_x$) coincides with the sign

178   of B_z increases before a substorm onset and maximizes close to an onset (note that we use

179   5-minute averages for B_x and v_z). From Figure 3 one can also see that for both databases,

180   the lines look quite similar, they start at less than 5% difference at the beginning of the

181   growth phase (or, more precisely, one hour before an onset) and reach almost the same

182   maximal value of about 30%, which means almost twofold difference between the number

183   of substorms with the same sign of B_z and ($v_z \cdot B_x$) and the number of substorms with the

184   opposite signs of those. At the same time, there is a certain distinction in the behavior of

185   red and blue lines (for positive and negative B_z); while the blue lines show a gradual in-

186   crease during the whole period of one hour with a more steep rise in last ten minutes, the

187   red lines remain at approximately the same values during first 30-40 minutes of a growth

188   phase, and then steeply go down in the last 20 minutes before a substorm onset, change

189   sign and reach maximum close to an onset.

194   The above statistics allows one to conclude that 2/3 of magnetospheric substorms

195   start under the situation when magnetotail plasma sheet moves in the same direction (up

196   or down the ecliptic plane) due to both IMF B_x and solar wind v_z and since the number

197   of periods with correlated signs of B_z and ($v_z \cdot B_x$) increases notably before the substorm

198   onset, it is reasonable to admit that this signs correlation (which increases the asymmetry

199   of the magnetotail) can facilitate a substorm onset.

200   Here, it is important to compare our results with a traditional idea of substorm trig-

201   gering by northward IMF B_z turning [*Lyons et al.*, 1997], which has been strongly criti-

202   cized in the last ten years (see *Morley and Freeman* [2007]; *Freeman and Morley* [2009];

203   *Newell et al.* [2016]). The results of superposed epoch analysis for the IMF B_z are pre-

204   sented in Figure 4 separately for two groups of substorms: those with with the same sign

205   of IMF B_z and ($v_z \cdot B_x$) before onset, and those with with the opposite signs of IMF B_z

206   and ($v_z \cdot B_x$). The solid line in Figure 4 corresponds to all the events which have IMF

207   $B_z < -1$ nT and ($v_z \cdot B_x$) < 0 together with the events where IMF $B_z > 1$ nT and

208   ($v_z \cdot B_x$) > 0. The dashed line comprises the other two groups of substorms. The anal-

209   ysis is done for SUPERMAG data set (left panel) and for *Frey et al.* [2004] data set (right

210   panel), with similar results. Both plots show the IMF B_z turning northward, and thus, the
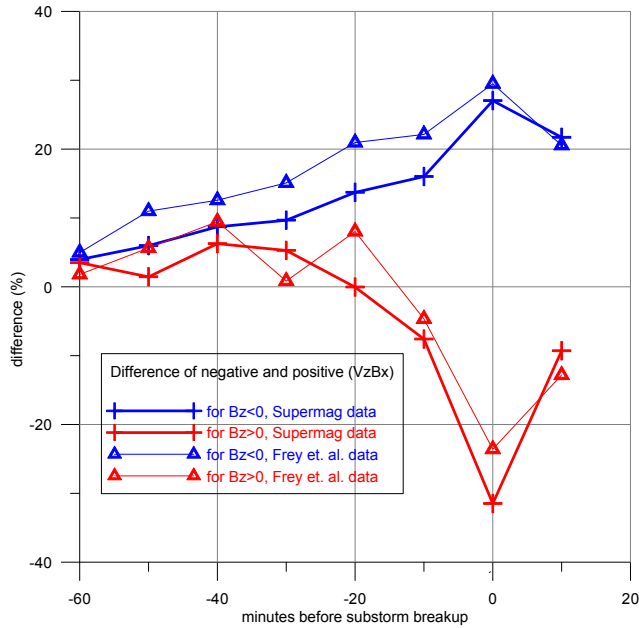
Figure 3. Time dependence of the difference between the number of the events when $(v_z \cdot B_x)$ was negative at a given time before onset, and the number of events when $(v_z \cdot B_x)$ was positive at the same time. Blue lines correspond to the substorm onsets under negative B_z, red lines to those under positive B_z, lines with triangles show Frey et.al. database, lines with crosses - SUPERMAG database.

substorm triggering by northward INF B_z turning is supported by our analysis. Also, both plots show smaller mean IMF B_z for the same sign substorms, given by solid lines. The smaller IMF B_z throughout the whole growth phase confirms our suggestions that these substorms start in average after lower energy input and thus would have lower substorm instability threshold.

4 $(v_z \cdot B_x)$ distribution in the Solar Wind

After we obtained the above signs correlation of B_z and $(v_z \cdot B_x)$ near a substorm onset, it is important to verify if the same correlation is a regular feature in the solar wind. For consistency, we analyzed the OMNI data for the similar (slightly widened) period, i.e. for the years 1996-2011. For the solar wind and the IMF components, we used the Geocentric Solar Ecliptic (GSE) frame, relevant for the solar wind studies. Again, for consistency, we used 5-minutes averages. For each year in this period (1996-2011) we analyzed the distributions of $(v_z \cdot B_x)$ for both positive $(B_z > 1$ nT$)$ and negative $(B_z < -1$ nT$)$ signs
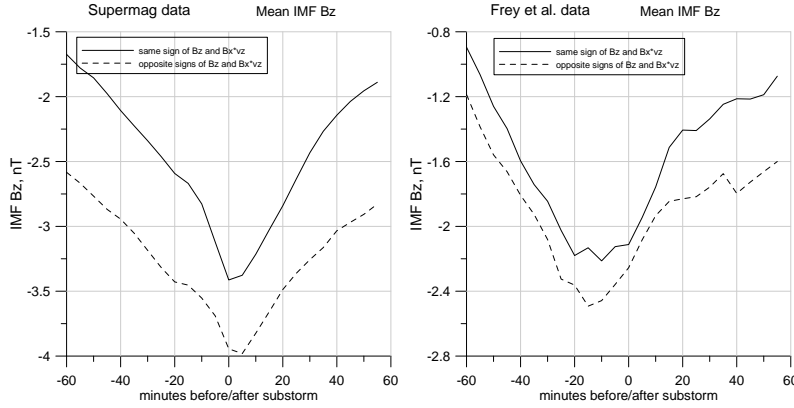
Figure 4. IMF B_z superposed epoch analysis for 2 different substorm classes, which are defined by the signs of IMF B_z and ($v_z \cdot B_x$) near the onset. Solid lines correspond to the ensemble means of substorms which started under the same sign of B_z and ($v_z \cdot B_x$), dashed lines - to those, which started under opposite B_z and ($v_z \cdot B_x$)

of IMF B_z. For all the 5-minutes periods during the given year when the IMF B_z was negative (< -1 nT) we calculated the number of 5-minute periods when ($v_z \cdot B_x$) was negative and the number of 5-minute periods when it was positive. The difference between these numbers (in percent) normalized by the whole number of 5-minute periods when IMF B_z was less than -1 nT, calculated for each year (a measure similar to that in Section 3), is plotted in Figure 5 with the blue line. After that, the same procedure was performed for the periods when the IMF B_z was positive (> 1 nT). The red line in Figure 5 shows the same relative difference, calculated for the periods, with IMF $B_z > 1$ nT. The Wolf Numbers are given in black for reference.

The resulting Figure 5 demonstrates the same type of imbalance as was obtained in Section 3. The values from the blue line are always positive; the red line gives only negative values (i.e., the number of periods with the same signs of the IMF B_z and ($v_z \cdot B_x$) is always greater than the number of periods with the opposite signs of those). In other words, the sign of the ($v_z \cdot B_x$) follows more often the sign of IMF B_z, rather than has the opposite sign. The degree of this imbalance varies with the solar cycle, it reaches maximal values (almost 50%, which means 3 times excess) soon after the solar maximum, and becomes much smaller (about 10-15%) at solar minimum. It is interesting to note that a
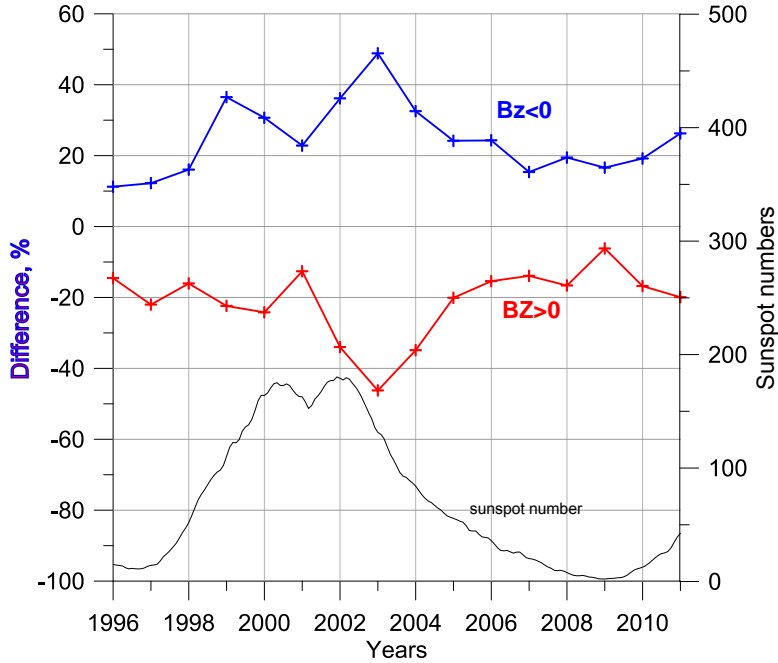
Figure 5. The normalized annual difference between the number of 5-minute periods with negative and positive $(v_z \cdot B_x)$ (in percent), calculated for the times when IMF B_z was less than -1 nT (blue line) or IMF B_z was greater than +1 nT (red line). The black line gives the sunspot numbers.

very similar behavior of the substorm occurrence rates throughout a solar cycle was reported in *Tanskanen* [2009].

5 Discussion and Conclusions

Our analysis showed that almost twice larger number of substorms onsets are observed in the periods when the IMF and SW parameters B_z and $(v_z \cdot B_x)$ have the same signs, if compared to the periods when those signs are opposite. These are the periods when the magnetotail plasma sheet is forced to move in the same direction (up or down from the ecliptic plane) due to both, the solar wind flow velocity and the interplanetary magnetic field B_x-component. We also showed that the difference between the number of events with positive and negative values of of $(v_z \cdot B_x)$ increases during the period of a growth phase, which may be interpreted as an additional trigger for a substorm onset. Indeed, if the number of occurrences of $(v_z \cdot B_x)$ with a proper sign (the same as the IMF B_z has) increases closer to an onset, it means that either v_z or B_x changes sign, which results in the enhancing of the plasma sheet displacement.

The statistical analysis of solar wind v_z and IMF B_x and B_z, provided in this study, shows that in the solar wind, also, the sign of the $(v_z \cdot B_x)$ follows more often the sign of IMF B_z, rather than has the opposite one.

A simple interpretation of these results implies that the imbalance in the number of periods with different signs of $(v_z \cdot B_x)$ is produced due to the Alfvén-type disturbances, propagating from the Sun. The importance and geo-effectiveness of Alfvén waves were discussed in a great number of papers, see *Belcher and Davis* [1971]; *Snekvik et al.* [2013]; *Zhang et al.* [2014], and references therein. Indeed if we assume that the undisturbed solar wind flows radially with V_{0x} velocity in the Sun-Earth direction (i.e. along the X_{GSE}-axis) and that the IMF background component is also radial and equals to B_{0x}, then, for a plane Alfvén-type wave disturbances (**b** and **v**) propagating along the Sun-Earth line (along the X_{GSE} axis):

$$\mathbf{b} = \mathbf{b}(x + ut) \quad \text{and} \quad \mathbf{v} = \mathbf{v}(x + ut) \,. \tag{1}$$

Here u is the wave velocity in a fixed frame of reference related to Earth, so that

$$u = \pm v_A + |V_{0x}|, \tag{2}$$

where v_A is the Alfvén velocity, and signs '+' and '−' correspond to anti-sunward and sunward directions, respectively. The linearized equation of motion then will look like (for Alfvén-type wave we also put total pressure gradient equal zero: $\nabla P = 0$) :

$$\rho \cdot \left(\frac{\partial \mathbf{v}}{\partial t} + V_{0x}\frac{\partial \mathbf{v}}{\partial x}\right) = \frac{1}{4\pi} \cdot \left(B_{0x}\frac{\partial \mathbf{b}}{\partial x}\right) \,. \tag{3}$$

where ρ is the plasma mass density. Note, that V_{0x} here is negative, so $V_{0x} = -|V_{0x}|$. Using (2), we substitute (1) to equation (3) and get

$$\rho\left(\frac{\partial \mathbf{v}}{\partial x}\right) = \pm\frac{1}{4\pi v_A} \cdot B_{0x}\left(\frac{\partial \mathbf{b}}{\partial x}\right) \,. \tag{4}$$

Equation (4) yields the following relationship between the velocity and magnetic field perturbations:

$$\rho \cdot \mathbf{v} = \pm\frac{1}{4\pi v_A} \cdot B_{0x} \cdot \mathbf{b} \,, \tag{5}$$

or, for the z-components (and after multiplying by B_{0x}):

$$\rho \cdot (v_z \cdot B_{0x}) = \pm\frac{1}{4\pi v_A} \cdot B_{0x}^2 \cdot b_z \,. \tag{6}$$

From the equation (6) one can see that in the case of earthward (anti-sunward) propagating waves the product ($\tilde{v}_z \cdot B_{0x}$) has the same sign as $\tilde{b}_z$-component.

If the Alfvén-type disturbances are born away from the Sun, we expect to observe two waves: directed to and from the Sun. If the disturbances appear near the Sun, where the plasma flow velocities are smaller than the Alfvén velocity, we will observe only one wave, directed earthward. Thus, the excess number of periods with correlated signs of the IMF B_z and ($v_z \cdot B_x$), reported in Section 4, probably, corresponds to the near-Sun-born disturbances. Since the more active Sun produces larger amount of Alfvén-type waves, the portion of ($v_z \cdot B_x$) with the sign of B_z changes from $\sim 3/4$ (difference 50% in Figure 4) in the years of the solar maximum to $\sim 9/11$ (10% difference in Figure 4) during the solar minimum.

These Alfvén-type disturbances (propagating earthward) more effectively shift and displace the magnetospheric plasma sheet and break the magnetospheric configuration symmetry, which, in turn, may facilitate a substorm onset.

Based on our findings, we summarize the results in the following items:

1. The number of substorms, which started when the solar wind and IMF components product ($v_z \cdot B_x$) had the same sign as the IMF B_z was about twice larger than the number of substorms with the opposite signs of those at the time of an onset. This tendency was proved on two substorm onset lists, obtained by different methods.

2. The analysis of pre-substorm changes in the number of periods with different signs of ($v_z \cdot B_x$) shows that the number of periods with preferable sign (same as B_z at breakup) increases progressively during a growth phase and reaches its maximum in the last 5 minutes near the onset. This effect is especially notable for the substorms, which start under positive B_z, which means that not only B_z, but also ($v_z \cdot B_x$) changes its sign before an onset

3. 11-years statistics shows that similar imbalance exists in the solar wind. The product ($v_z \cdot B_x$) has the same sign as B_z during 2/3 of all the time if we take the whole solar cycle period. This portion increases to 3/4 during the years near the solar maximum, and decreases to 9/11 in a years near the minimum of solar activity.

The last conclusion leads to a suggestion that the ($v_z \cdot B_x$) value may be an important agent in substorm initiation, forcing an earlier breakup by changing plasma sheet motion

320 direction. This suggestion needs further and more detailed (case) investigations of sub-
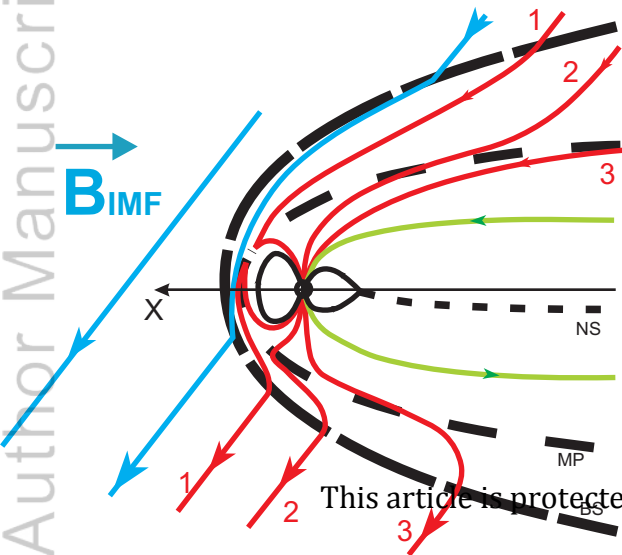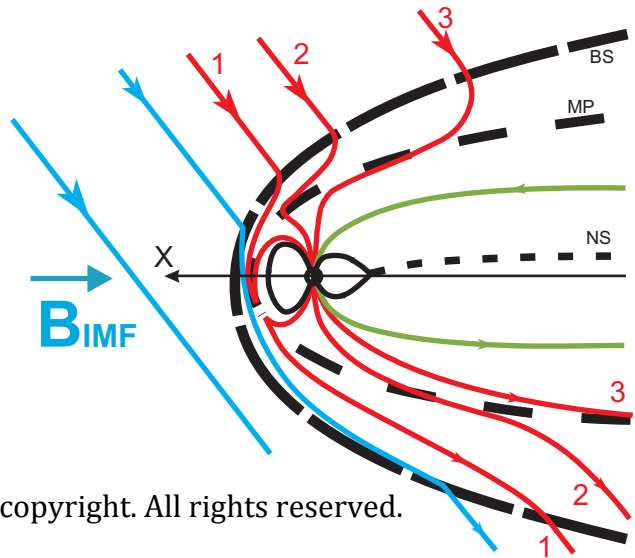
321 storm dynamics.

Acknowledgments

References

336 Akasofu, S. I. (1975), Roles of north-south component of interplanetary magnetic-field on

337 large-scale auroral dynamics observed by DMSP satellite, *Planet. Space Sci.*, *23*, 1349-

338 1354.

339 Belcher, J. W., and L. Davis (1971), Large-amplitude Alfveń waves in the interplanetary

340 medium, 2, *J. Geophys. Res.*, *76*, 3534Ű3563.

341 Borovsky, J. E., and K. Yakymenko (2017),Substorm occurrence rates, substorm

342 recurrence times, and solar wind structure, *J. Geophys. Res.*, *122*, 2973-2998,

343 doi:10.1002/2016JA023625.

344 Cowley S.W.H. (1981), Asymmetry effects associated with the x-component of the IMF in

345 a magnetically open magnetosphere, *Planet. Space Sci.*, *29*, 8, 809-818.

346 Dungey, J. W. (1961), Interplanetary magnetic field and the auroral zones. *Phys. Rev. Lett.*,

347 *6*, 47Ű48.

348 Fairfield, D. H., and J. L. J. Cahill (1966), Transition region magnetic field and polar

349 magnetic disturbances, *J. Geophys. Res.*, *71*,1, 155Ű169.

Freeman,M.P.,and S.K.Morley (2009), No evidence for externally triggered substorms based on superposed epoch analysis of IMF Bz. Geophys.Res.Lett.36,L21101. http://dx.doi.org/10.1029/2009GL040621.

Frey, H. U., S. B. Mende, V. Angelopoulos, and E. F. Donovan (2004), Substorm onset observations by IMAGE-FUV, *J. Geophys. Res.*, *109*, A10304, doi:10.1029/2004JA010607.

Gordeev, E.I., Sergeev, V.A., Amosova, M.V., Andreeva V.A. (2016), Influence of interplanetary magnetic field radial component on the position of the Earth's magnetotail neutral sheet, *Geophysical methods of survey the Earth and its subsoil*, 11-21, doi:10.13140/RG.2.1.4821.6565

Hoilijoki, S., V. M. Souza, B. M. Walsh, P. Janhunen, and M. Palmroth (2014), Magnetopause reconnection and energy conversion as influenced by the dipole tilt and the IMF Bx , J. Geophys. Res. Space Physics, 119, doi:10.1002/2013JA019693

Kivelson, M.G., W.J. Hughes (1990), On The Threshold For Triggering Substorms,*Planet. Space Sci.*, *38*, 2, 211-220.

Kubyshkina, M., N. Tsyganenko, V. Semenov, D. Kubyshkina, N. Partamies and E. Gordeev (2015), Further evidence for the role of magnetotail current shape in substorm initiation, *Earth, Planets and Space*, *67*, 139, doi:10.1186/s40623-015-0304-1, 2015

Lyons,L.R.,G.T.Blanchard,J.C.Samson,R.P.Lepping,T.Yamamoto, and T. Morreto (1997), Coordinated observations demonstrating external substorm triggering. *J. Geophys. Res.*, *102*, A12, doi:10.1029/97JA02639.

Morley,S.K., and M.P.Freeman (2007), On the association between northward turnings of the interplanetary magnetic field and substorm onsets, *Geophys.Res.Lett.*, *34*, L08104. doi:10.1029/2006GL028891.

P.T.Newell, K.Liou, J.W.Gjerloev, T.Sotirelis, S.Wing, E.J.Mitchell(2016), Substorm probabilities are best predicted romsolar wind speed, *Journal of Atmospheric and Solar-Terrestrial Physics*,*146*, 28Ű37, doi:10.1016/J.JASTP.2016.04.019

Panov, E.V., R. Nakamura, W. Baumjohann, M. Kubyshkina, A. V. Artemyev, V. A. Sergeev, A. A. Petrukovich, V.Angelopoulos, K.-H. Glassmeier, J. P. McFadden and D. Larson(2012) Kinetic ballooning/interchange instability in a bent plasma sheet, *J. Geophys. Res.*, *117*, A06228, doi: 10.1029/2011JA017496.

Reistad, J. P., N. Östgaard, K. M. Laundal,S. Haaland, P. Tenfjord, K. Snekvik,K. Oksavik, and S. E. Milan (2014), Intensity asymmetries in the dusk sector of the pole-

Confidential manuscript submitted to *Geophysical Research Letters*

ward auroral oval due to IMF Bx , *J. Geophys.Res. Space Physics*, *119*, 9497-9507, doi:10.1002/2014JA020216

Rostoker, G., and C. G. Falthammar (1967), Relationship between changes in the interplanetary magnetic field and variations in the magnetic field at EarthŠs surface, *J. Geophys. Res.*, *72*, 5853.

Semenov, V.S., D.I. Kubyshkina, M.V. Kubyshkina, I.V. Kubyshkin, and N. Partamies (2015), On the correlation between the fast solar wind flow changes and substorm occurrence, *Geophysical Research Letters*,*42*, 13, 5117-5124, doi:10.1002/2015GL064806.

Sergeev, V. A., N. A.Tsyganenko, and V.Angelopoulos (2008), Dynamical response of the magnetotail to changes of the solar wind direction: an MHD modeling perspective, *Ann. Geophys.*, *26*, 2395-2402, doi:10.5194/angeo-26-2395-2008.

Shue, J.-H., P. T. Newell, K. Liou, C. Meng, and S. W. H. Cowley (2002), Interplanetary magnetic field Bx asymmetry effect on auroral brightness, *J. Geophys. Res.*, *107*, SIA 16-1, doi:10.1029/2001JA000229.

Snekvik K., E. I. Tanskanen, and E.K.J.Kilpua(2013), An automated identification method for Alfvénic streams and their geoeffectiveness, *J. Geophys. Res.*, *118*, 5986Ű5998, doi:10.1002/jgra.5058.

Tanskanen E. I. (2009), A comprehensive high-throughput analysis of substorms observed by IMAGE magnetometer network: Years 1993Ű2003 examined, *J. Geophys. Res.*, *114*, doi:10.1029/2008JA013682

Tsyganenko, N. A., and D. H. Fairfield (2004), Global shape of the magnetotail current sheet as derived from Geotail and Polar data, *J. Geophys. Res.*, *109*, A03218, doi:10.1029/2003JA010062.

Vörös, Z., G. Fasko, M. Khodanchenko, I. Honkonen, P. Janhunen, and M. Palmroth 312 (2014) Windsock memory COnditioned RAM (CO-RAM) pressure effect: Forced re- 313 connection in the Earth's magnetotail, *J.Geophys.Res.*,*119*, 6273-6293, 314, doi:10.1002/2014JA019857

Zhang, X.-Y., M. B. Moldwin, J. T. Steinberg, and R. M. Skoug (2014), Alfvén waves as a possible source of long-duration, large-amplitude, and geoeffective southward IMF, *J. Geophys. Res.*, *119*, 3259Ű3266, doi:10.1002/2013JA019623.
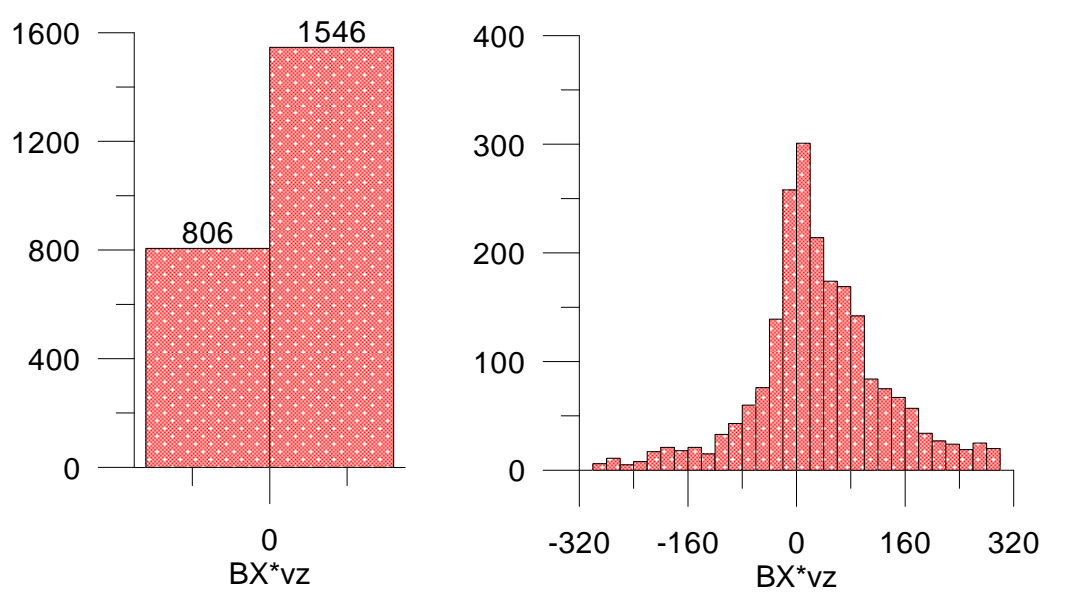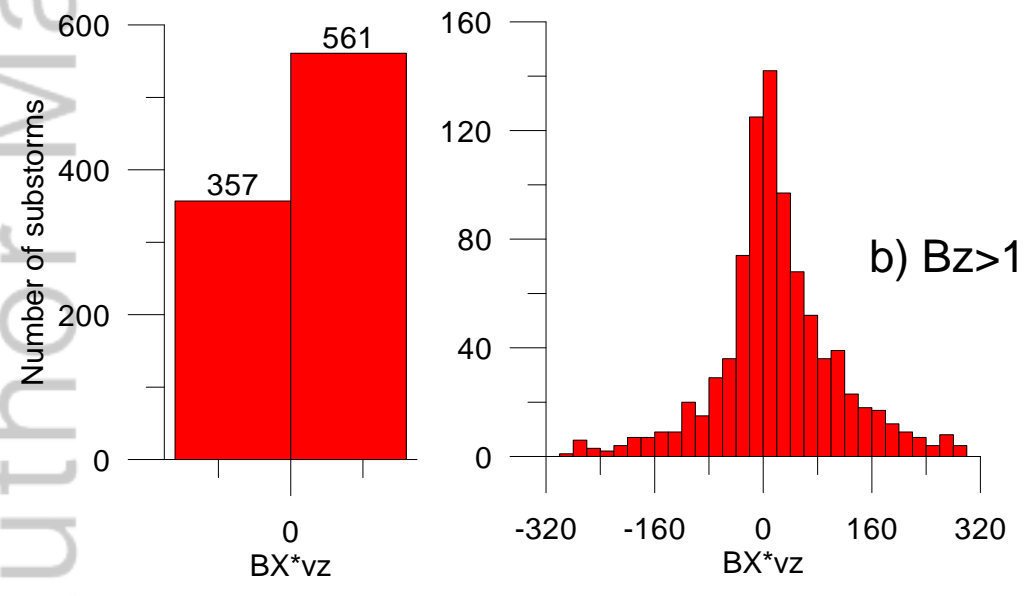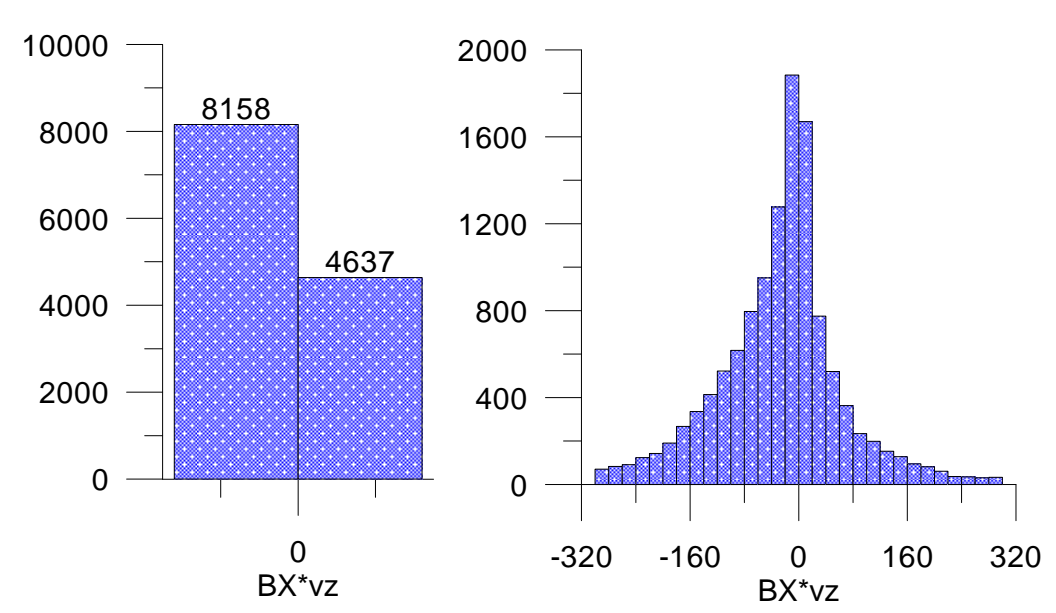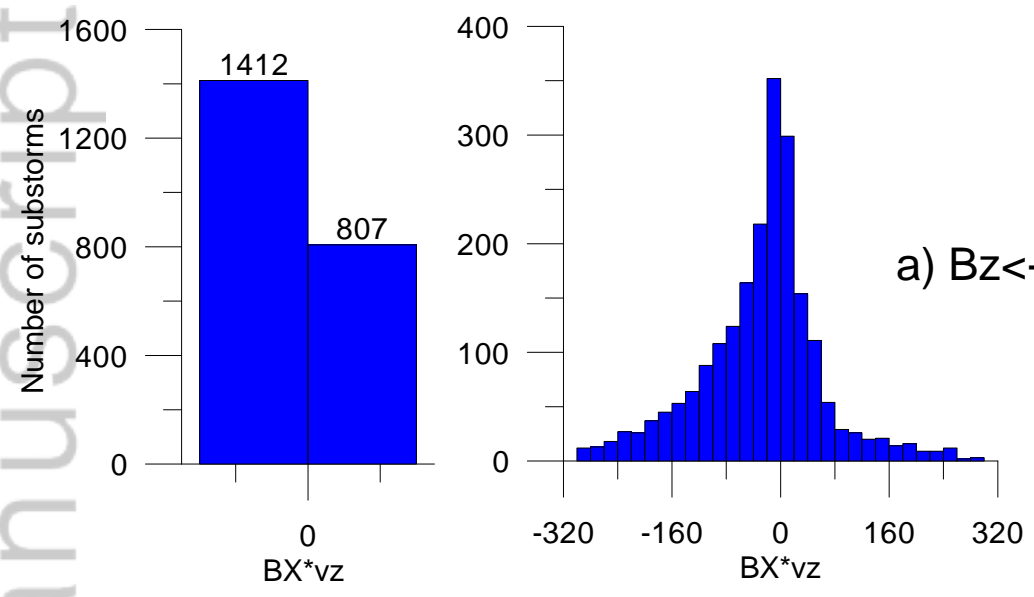
Figure 1.

IMF Bx>0

IMF Bx<0

B_{IMF}

B_{IMF}

Figure 2.

a) Bz<-1nT

b) Bz>1 nT

Frey et al. substorm data

SUPERMAG substorm data

Figure 3.

difference (%)

minutes before substorm breakup

Difference of negative and positive (VzBx)

— for Bz<0, Supermag data
— for Bz>0, Supermag data
△ for Bz<0, Frey et. al. data
△ for Bz>0, Frey et. al. data
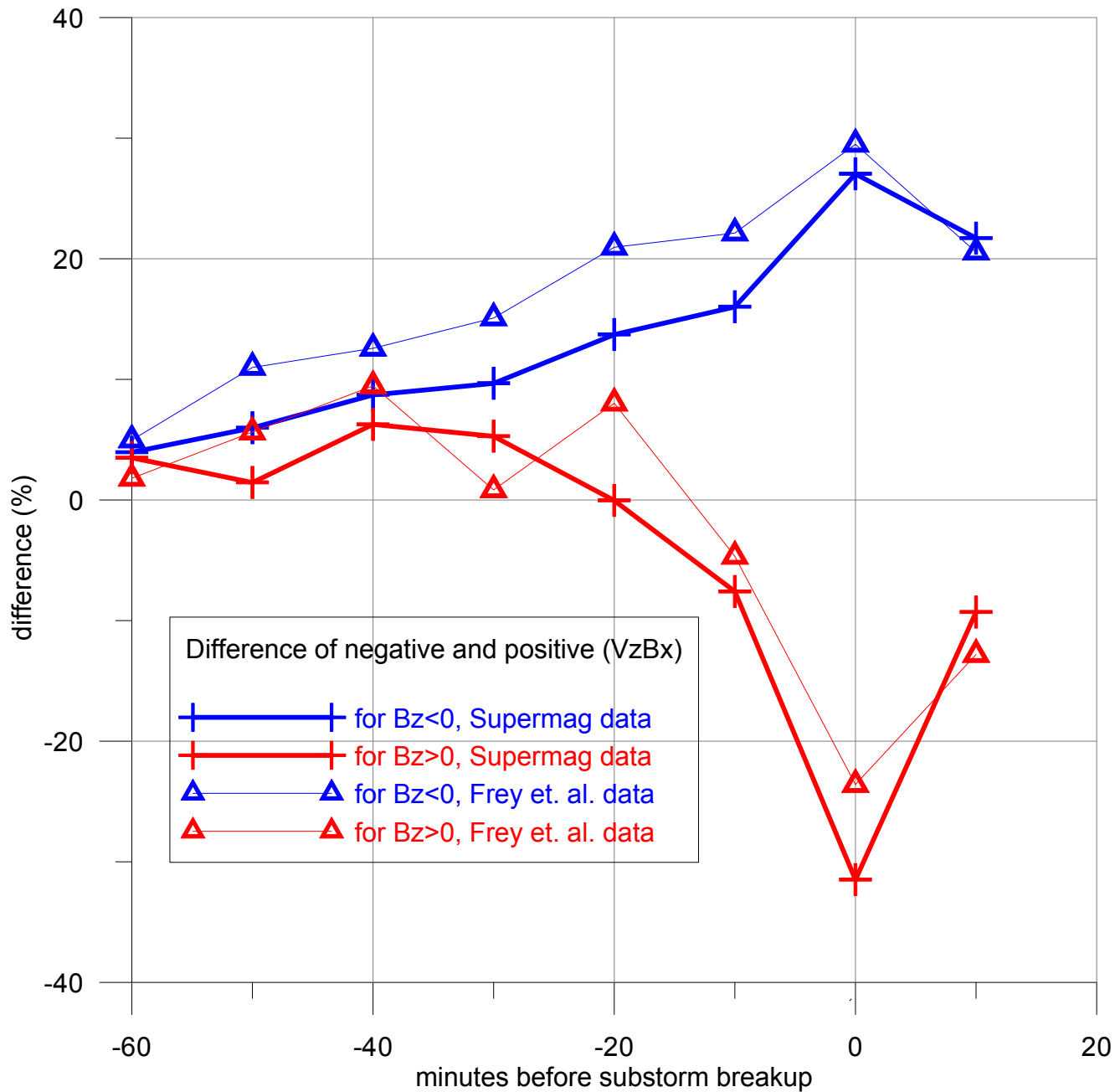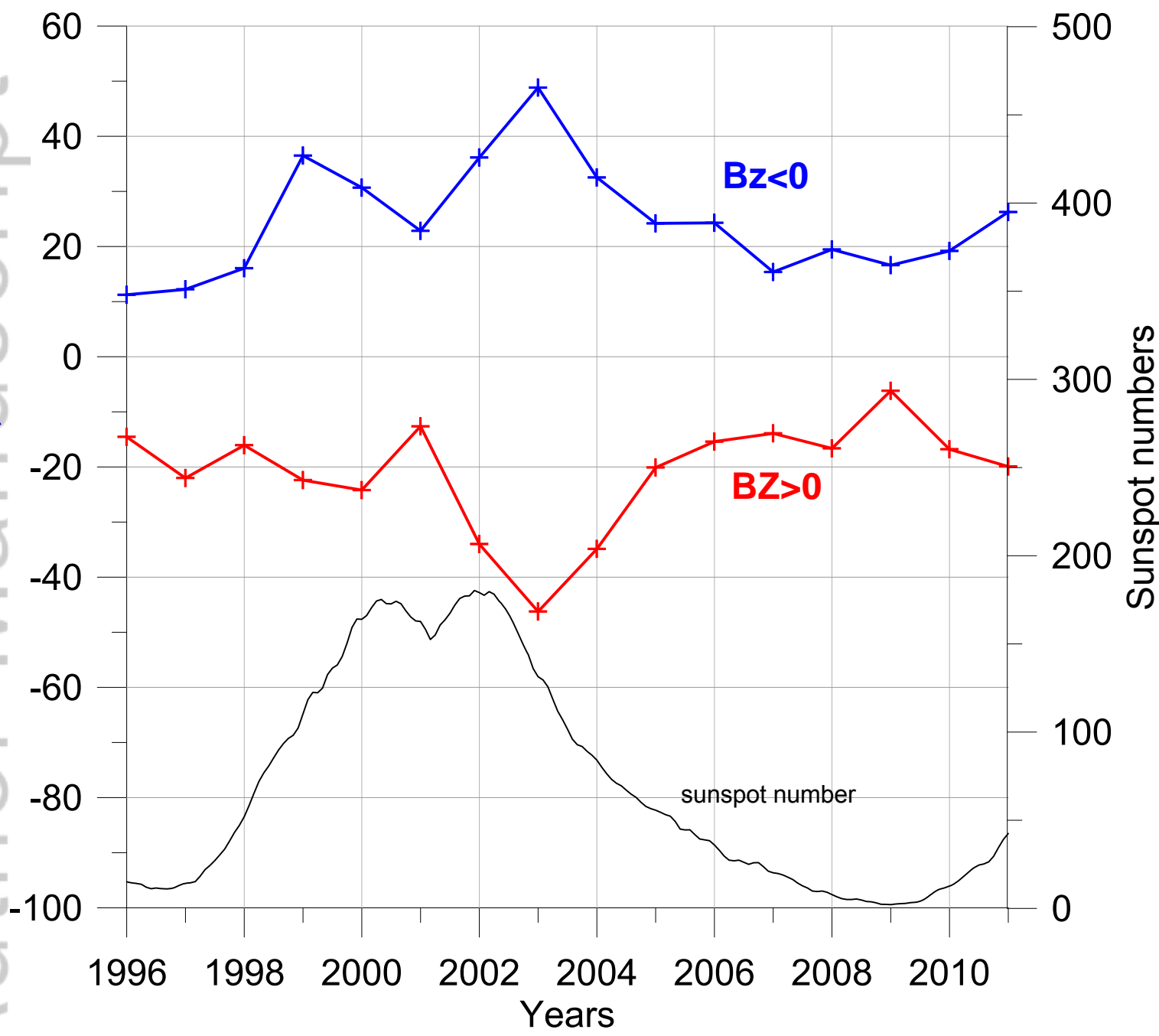
Figure 5.

Figure 4.

Supermag data — Mean IMF Bz

IMF Bz, nT vs. *minutes before/after substorm*

— same sign of Bz and Bx*vz
-- opposite signs of Bz and Bx*vz
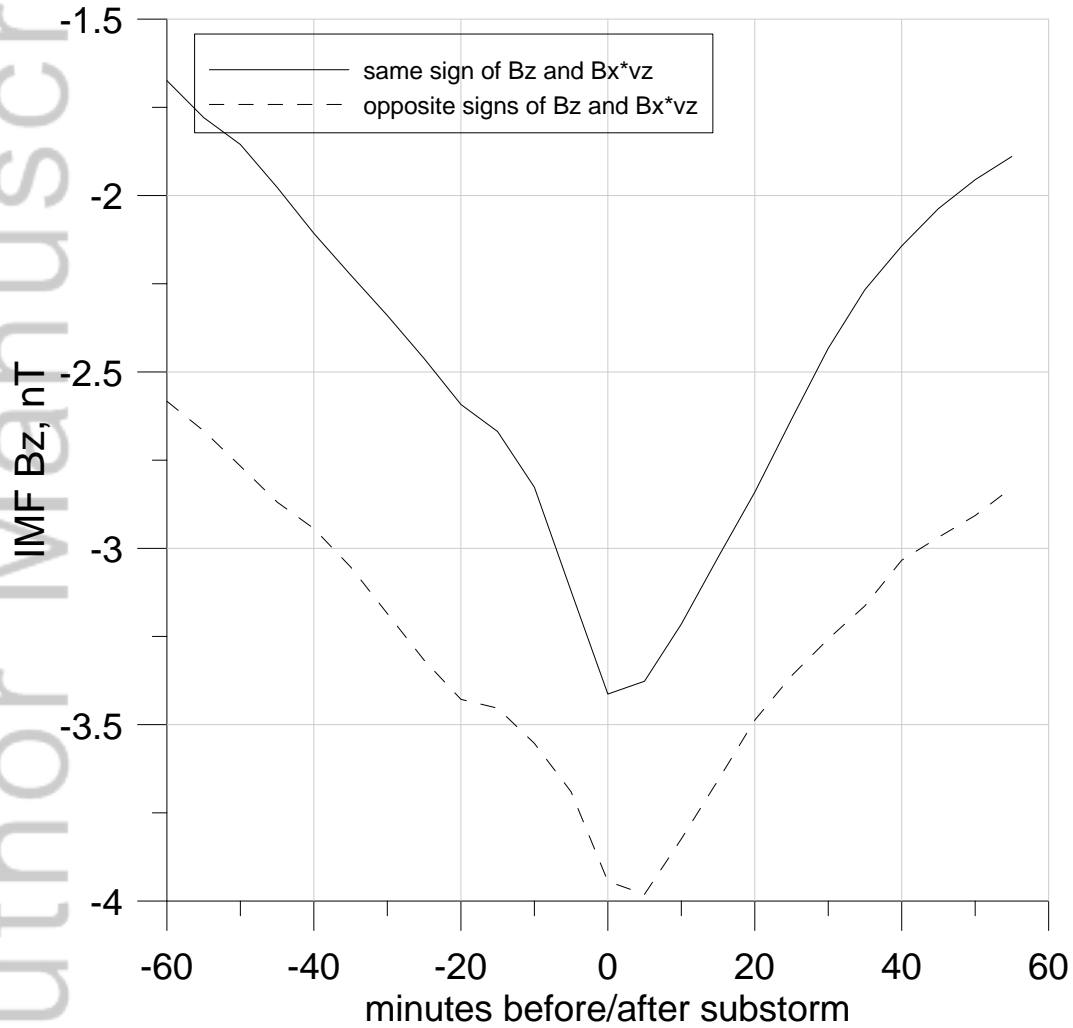
Frey et al. data — Mean IMF Bz

IMF Bz, nT vs. *minutes before/after substorm*

— same sign of Bz and Bx*vz
-- opposite signs of Bz and Bx*vz